

Magnetic Resonance Imaging with Diffusion in Differentiation between Spinal Canal Lesions

Yassmin Abd El Azeem Sakr^{1*}, Esam AbdElhay Mokbel², Rasha Lofty Younes¹ Samah Ahmed Radwan¹

¹ Radiodiagnosis Department, ² Neurosurgery Department, Faculty of Medicine, Tanta University, Tanta, Egypt

*Corresponding Author: Yassmin Abd El Azeem Sakr, Email: yassminsakr455@gmail.com, mobile: +201557757726

ABSTRACT

Background: Diffusion weighted imaging (DWI) offers distinct contrast information, which complements the data obtained from conventional magnetic resonance imaging (MRI) by detecting microstructural alterations.

Objective: This work aimed to evaluate the role of MRI with DWI in differentiation between variant spinal canal lesions.

Individuals and methods: This prospective work was conducted on 30 individuals of both sexes with neurological symptoms and spinal canal pathology (back pain, pressure in neck, back or head, weakness, numbness and tingling or loss of sensation in hands, fingers, or feet). MRI and DWI-MRI are assessed for all patients.

Results: Area under curve (AUC) of 0.972 and an apparent diffusion coefficient (ADC) cutoff of ≤ 1.25 could predict malignant lesions with 88.5% sensitivity and 92.4% specificity. Malignant lesion had statistically significant higher diffusion restriction as appeared from the DWI and from the ADC ($p < 0.001$). No statistically substantial variations had been existed in the lesion site ($p = 0.16$) T1 ($p = 0.081$) or T2 ($p = 0.607$) appearance. Patients with malignant masses had higher mean age, however, without statistical significance ($p = 0.379$). No statistically substantial variation had been noted in the sex distribution, or the clinical presentation.

Conclusions: Spinal canal lesions encompass a wide range of neoplastic and non-neoplastic conditions, posing diagnostic challenges due to their often-similar appearance on routine MRI sequences.

Keywords: Apparent diffusion coefficient, Diffusion weighted imaging, Magnetic resonance imaging, Spinal canal lesions.

INTRODUCTION

Spinal canal lesions can be categorized as neoplastic and non-neoplastic. The non-neoplastic lesions include vascular, inflammatory, developmental, demyelinating, degenerative, metabolic, and toxic disorders^[1]. The neoplastic lesions are also classified according to their location (inside or outside the spinal cord) as extradural, intradural extramedullary, and intradural intramedullary^[2].

Extradural tumours are commonly metastatic that spread from cancer located in another part of the body^[3]. The intradural-extramedullary grows inside the dura but outside of the spinal cord^[4].

Magnetic resonance imaging (MRI) allows for the assessment of both soft tissue and bone structures^[5]. MRI of the spine is the primary imaging technique used to diagnose disorders due to its ability to provide sufficient contrast resolution, allowing for differentiation of intraspinal soft tissue structures and identification of spinal cord or canal abnormalities^[6]. MRI provides superior distinction of soft tissues compared to computed tomography (CT) and other radiography. This enables more accurate characterisation of the spinal cord, discs, ligaments, arteries, and other soft tissue structures inside the spinal canal^[7].

DWI offers distinct contrast information that complements the information obtained from standard MRI by detecting microstructural alterations^[8]. It enhances MRI scans by including functional data with the primarily anatomical data obtained via standard sequences^[9].

One of the most beneficial uses of DWI outside of the

skull is for assessing the spine. DWI may aid in the identification and characterisation of intramedullary, intradural-extramedullary, and epidural lesions. DWI might help distinguish between the occurrence of alterations due to inflammation, neoplasms, infections, and ischemia. DWI enhances the ability to identify and detect the existence of osseous, bone metastases and myeloma^[10].

The functioning of DWI mostly relies on the tissue microstructure that determines water molecules random movement known as Brownian motion. In a proportional connection, signal attenuation accurately represents the intensity of water movement. The ADC value is determined utilizing maps obtained from diffusional signal attenuation, enabling the measurement of Brownian motion^[11].

Tissues that contain a significant amount of water that is not bound to other molecules, including those with low amounts of membranes and intracellular organelles or large amounts of freely available extracellular water, may exhibit lower signal intensity on DWI and greater signal intensity on ADC imaging^[12]. This work aimed to evaluate the role MRI with DWI in differentiation between variant spinal canal lesions.

PATIENTS AND METHODS

This prospective work was performed on 30 instances of both sexes, with neurological symptoms and spinal canal pathology (back pain, pressure in neck, back or head, weakness, numbness and tingling or loss of sensation in hands, fingers, or feet).

Exclusion criteria: People who are contraindicated for MRI including those with metallic implants such as pacemakers, aneurysm clips, or other electronic or magnetically actuated implants, in addition to people who experience claustrophobia, patients with congenital spinal disorders and patients with spinal trauma or previous spinal operation.

Each participant had a comprehensive evaluation, which included obtaining their history, performing a thorough clinical examination, and executing an MRI examination utilizing a 1.5 T MRI GE (General Electric) machinery. Histopathology examination [for the lesion if patient did excision biopsy].

Routine MRI pulse sequences was included:

Sagittal T2WFSE: TR/TE: 2245/101, FOV: 33×33, 4 mm thickness, NEX: 4 and matrix: 320* 224.

Sagittal T1WFSE: TR/TE: 340-560/9-10, FOV: 33×33, 4 mm thickness, NEX: 4 and matrix: 320* 224.

Axial T1: TR/TE: 424-524/3-7, FOV: 33×33, 4 mm thickness, NEX: 4 and matrix: 320* 224.

Axial T2:TR/TE: 2230/101-150, FOV: 33×33, 4 mm thickness, NEX: 4 and matrix: 320* 224.

Proton Density-Weighted Spin Echo Images: PDSE (TR >1000 msec); TE are produced by using both long TR and short TE, and they provide a signal that represents the proton density in the imaging field.

Inversion Recovery (STIR): When using inversion recovery (TR >2000 msec, TE30 msec, TI = 120-150 msec), a fat saturation method, the signal intensity from fat is significantly reduced, while the signal from fluid and oedema is noticeably enhanced. This approach was formerly known as short time inversion recovery (STIR) imaging.

Contrast study T1 for the cases that are suspected to be inflammatory or neoplastic in nature.

Diffusion weighted MR imaging (DWI-MRI): DWI imaging sequence used a single-shot spin echo EPI sequence with specific parameters, including a TR of 1600 ms, TE of 95 ms, and NEX of 1. The FOV was 40 x 20 cm, with a matrix size of 176 x 256. The slice thickness was 5 mm, with a 1 mm inter-slice gap. The diffusion sensitivities were established at b values of 0 and 1000 s/mm² squared. To acquire images of the spine, a standard phased array surface receiver coil was utilized.

The Apparent Diffusion Coefficient (ADC) maps: The ADC value is often represented as ×10⁻³ mm²/s. A monoexponential model is used to automatically build an ADC map on a pixel-by-pixel or voxel-by-voxel basis. Next, the radiologist might delineate a region of interest (ROI) inside the specific tissue of interest in order to acquire a precise quantitative measurement. Usually, the ROI yields automatically produced ADC values, such as the minimal, mean, and maximum

values, or a mean value accompanied by a range in parenthesis.

Imaging assessment: The structural aspects of each abnormality were documented, including its signal properties and the way it appeared after contrast enhancement.

Analysis of diffusion weighted images and calculating the ADC: The presence of the lesion was identified on DWI and ADC map, with the use of conventional MR images as a reference. - The signal intensity of the lesion on DWIs was assessed. - The ADC was measured utilizing an electronic cursor on the ADC map in various ROI inside the lesion. - Regions exhibiting flow void, calcification, or dense fibrosis, as well as normal tissue, were deliberately excluded when selecting the ROI. A ROI in the shape of an ellipse was positioned on the portion of a solid tumor that exhibited the lowest ADC value on the ADC maps. - The average value was determined by ADC. The ADC value is useful for distinguishing between benign and malignant lesions of the spine.

Ethical approval: The work was performed following approval from the Ethics Committee of Tanta University Hospitals, Tanta, Egypt. The patients or relatives of the patients provided a well-informed written consents. The Declaration of Helsinki was followed through the study conduction. The Declaration of Helsinki was followed through the study conduction.

Statistical analysis

The statistical analysis was conducted using SPSS version 26 software (IBM Inc., Chicago, IL, USA). The quantitative parameters were expressed as the mean and standard deviation (SD) and contrasted between both groups utilizing an unpaired Student's t-test. The qualitative parameters were shown as frequencies and percentages (%) and examined using the Chi-square or Fisher's exact test, as applicable. The study utilized Receiver Operating Characteristic (ROC) analysis to determine the overall predictive ability of a parameter and identify the optimal cut-off value. This analysis also allowed for the assessment of sensitivity and specificity at the chosen cut-off value. A two-tailed P value ≤ 0.05 was considered statistically significant.

RESULTS

The mean age was 50.73 ± 13.41 years. 14 (46.7%) patients were females and 16 (53.3%) were males. The most prevalent clinical presentation was back pain 28 (93.3%) followed by 15 (50%) numbness, and 11 (36.7%) limb weakness. Other symptoms were headache 2 (6.7%), bowel and bladder dysfunction 1 (3.3%), 1 (3.3%) blurred vision, 1 (3.3%) fever and 1 (3.3%) neck stiffness (Table 1).

Table (1): Distribution of the studied cases based on demographic data, clinical presentation.

		N=30
Age (years)		50.73 ± 13.41
Sex	Female	14(46.7%)
	Male	16(53.3%)
Clinical presentation		
Back Pain		28(93.3%)
Numbness	Right	6(20.0%)
	Left	7(23.3%)
	Bilateral	2(6.7%)
Limb weakness	Right	5(16.7%)
	Left	4(13.3%)
	Bilateral	2(6.7%)
Bowel and bladder dysfunction		1(3.3%)
Headache		2(6.7%)
Blurred vision		1(3.3%)
Fever		1(3.3%)
Neck stiffness		1(3.3%)

Data are presented as mean ± SD or frequency (%).

The lesions were found located lumbar in 11 (36.7%) patients, cervical in 10 (33.3%) patients, dorsal in 6 (20.0%) patients, lumbosacral in 2 (6.7%), and sacrococcygeal in 1 (3.3%). Most of the lesions were hypointense in T1 in 20 (66.7%) patients, hyperintense in T2 in 4 (13.3%) patients and DWI in 14 (46.7%) patients. The mean of ADC was 0.49 ± 0.13 (Table 2).

Table (2): MRI characteristics of the studied lesions

		N=30
Lesion site	Cervical	10(33.3%)
	Dorsal	6(20.0%)
	Lumbar	11(36.7%)
	Lumbosacral	2(6.7%)
	Sacrococcygeal	1(3.3%)
T1 appearance	Hyperintense	4(13.3%)
	Hypointense	20(66.7%)
	Isointense	5(16.7%)
	Mixed	1(3.3%)
T2 appearance	Hyperintense	13 (43.3%)
	Hypointense	9(30.0%)
	Isointense	3(10.0%)
	Mixed	5(16.7%)
DWI appearance	Hyperintense	14(46.7%)
	Hypointense	10(33.3%)
	Isointense	5(16.7%)
	Mixed	1(3.3%)
ADC (10-3 mm²/s)		1.38 (1.15 – 1.83)

Data are presented as frequency (%) or median (IQR), DWI: Diffusion Weighted Imaging, ADC: apparent diffusion coefficient.

There were 22 (73.3%) patients had benign lesions, while 8 (26.7%) patients had malignant lesions.

Concerning tissue types, the most common benign lesion was in 4 (13.3%) patients, and the most common malignant lesion was metastasis and was in 23.3% patients. The primary sites for metastasis were HCC in 2 (6.7%) patients, breast cancer in 1 (3.3%) patient, bronchogenic carcinoma in 1 (3.3%) patient, cancer colon in 1 (3.3%) patient, sinus melanoma in 1 (3.3%) patient, and thyroid carcinoma in 1 (3.3%) patients (Table 3).t

Table (3): Pathological diagnosis of the studied patients

		N=30	
Type of the lesion			
Benign	Abscess	1 (3.3%)	
	Disc bulge	5 (16.7%)	
	Ependymoma	1 (3.3%)	
	Hemangioma	4 (13.3%)	
	Meningioma	1 (3.3%)	
	Multiple sclerosis	2 (6.7%)	
	Neurofibroma	1 (3.3%)	
	Osteoporosis	3 (10.0%)	
	Schwannoma	1 (3.3%)	
	Spondylodiscitis	3 (10.0%)	
	Malignant	Chordoma	1 (3.3%)
		Metastasis	Breast cancer
Bronchogenic carcinoma			1 (3.3%)
Cancer colon			1 (3.3%)
HCC			2 (6.7%)
Sinus melanoma			1 (3.3%)
Thyroid cancer			1 (3.3%)

Data are presented as frequency (%), HCC: hepatocellular carcinoma.

Patients with malignant masses had higher mean age, however, without statistical significance (p=0.379). No statistically substantial variations had been noted in the sex distribution (p = 0.689), or the clinical presentation (p > 0.05) (Table 4).

Table (4): Comparison between patients with benign and malignant masses in the baseline demographic and clinical data

		Benign mass (n = 22)	Malignant mass (n = 8)	P
Age (years)		49.41 ± 13.79	54.38 ± 12.42	0.379
Sex	Female	11(50.0%)	3(37.5%)	0.689
	Male	11(50.0%)	5(62.5%)	
Clinical presentation	Back Pain	20(90.9%)	8(100.0%)	1.0
	Numbness	11(50.0%)	4(50.0%)	1.0
	Limb weakness	8(36.4%)	3(37.5%)	1.0
	Bowel and bladder dysfunction	0(0.0%)	1(12.5%)	0.267
	Headache	2(9.1%)	0(0.0%)	1.0
	Blurred vision	1(4.5%)	0(0.0%)	1.0
	Fever	1(4.5%)	0(0.0%)	1.0
	Neck stiffness	1(4.5%)	0(0.0%)	1.0

Data are presented as mean ± SD or frequency (%), *: Statistically significant at p ≤ 0.05.

Malignant lesion had statistically substantial higher diffusion restriction as appeared from the DWI (100% of cases restricted compared to a percentage 27.3% in the benign lesions, p < 0.001), and from the ADC (10-3 mm²/s) values (0.99 ± 0.14 compared to 1.62 ± 0.35 in benign lesions, p<0.001). No statistically substantial variations were existed in the lesion site (p = 0.16) T1 (p = 0.081) or T2 (p = 0.607) appearance (Table 5).

Table (5): Comparison between benign and malignant masses in the MRI data

		Lesion		P
		Benign (n = 22)	Malignant (n = 8)	
Site	Cervical	9(40.9%)	1(12.5%)	0.16
	Dorsal	3(13.6%)	3(37.5%)	
	Lumbar	8(36.4%)	3(37.5%)	
	Lumbosacral	2(9.1%)	0(0.0%)	
	Sacrococcygeal	0(0.0%)	1(12.5%)	
T1 appearance	Hyperintense	4(18.2%)	0(0.0%)	0.081
	Hypointense	13(59.1%)	7(87.5%)	
	Isointense	5(22.7%)	0(0.0%)	
	Mixed	0(0.0%)	1(12.5%)	
T2 appearance	Hyperintense	10(45.5%)	3(37.5%)	0.607
	Hypointense	6(27.3%)	3(37.5%)	
	Isointense	3(13.6%)	0(0.0%)	
	Mixed	3(13.6%)	2(25.0%)	
DWI appearance	Hyperintense	6(27.3%)	8(100.0%)	0.006*
	Hypointense	10(45.5%)	0(0.0%)	
	Isointense	5(22.7%)	0(0.0%)	
	Mixed	1(4.5%)	0(0.0%)	
ADC value (10⁻³ mm²/s)		1.62 ± 0.35	0.99 ± 0.14	<0.001*

Data are presented as frequency (%), *: Statistically significant at p ≤ 0.05, DWI: Diffusion weighted imaging, ADC: apparent diffusion coefficient.

ROC curve analysis was conducted to evaluate the accuracy of ADC values in differentiating malignant masses. The ADC values, expressed in ADC (10-3 mm²/s), demonstrated significant predictive power for malignant lesions (p < 0.001), with an area under the curve (AUC) of 0.972. ADC cutoff ≤ 1.25 could predict malignant lesions with (88.5%) sensitivity and (92.4%) specificity (Figure 1).

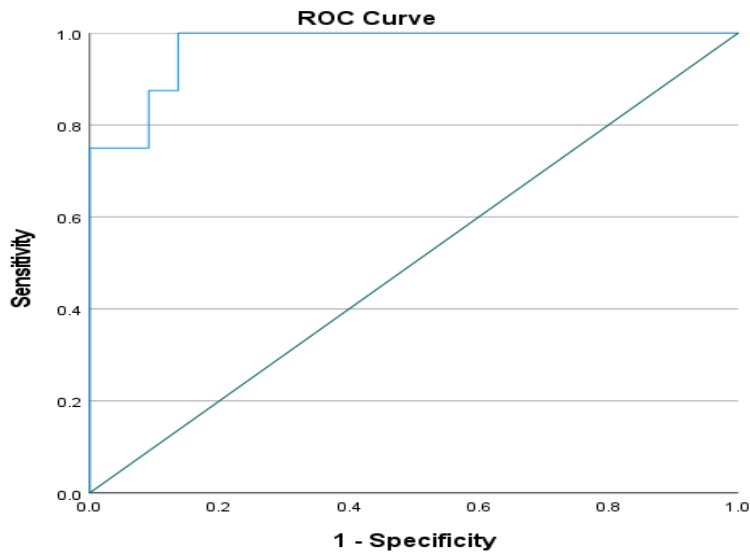


Figure (1): ROC curve for ADC to predict malignant masses.

CASE 1

45 years old female patient complaining from lower back pain and lack of bladder and bowel control. A case of chordoma with vertebral mets (Figure 2).

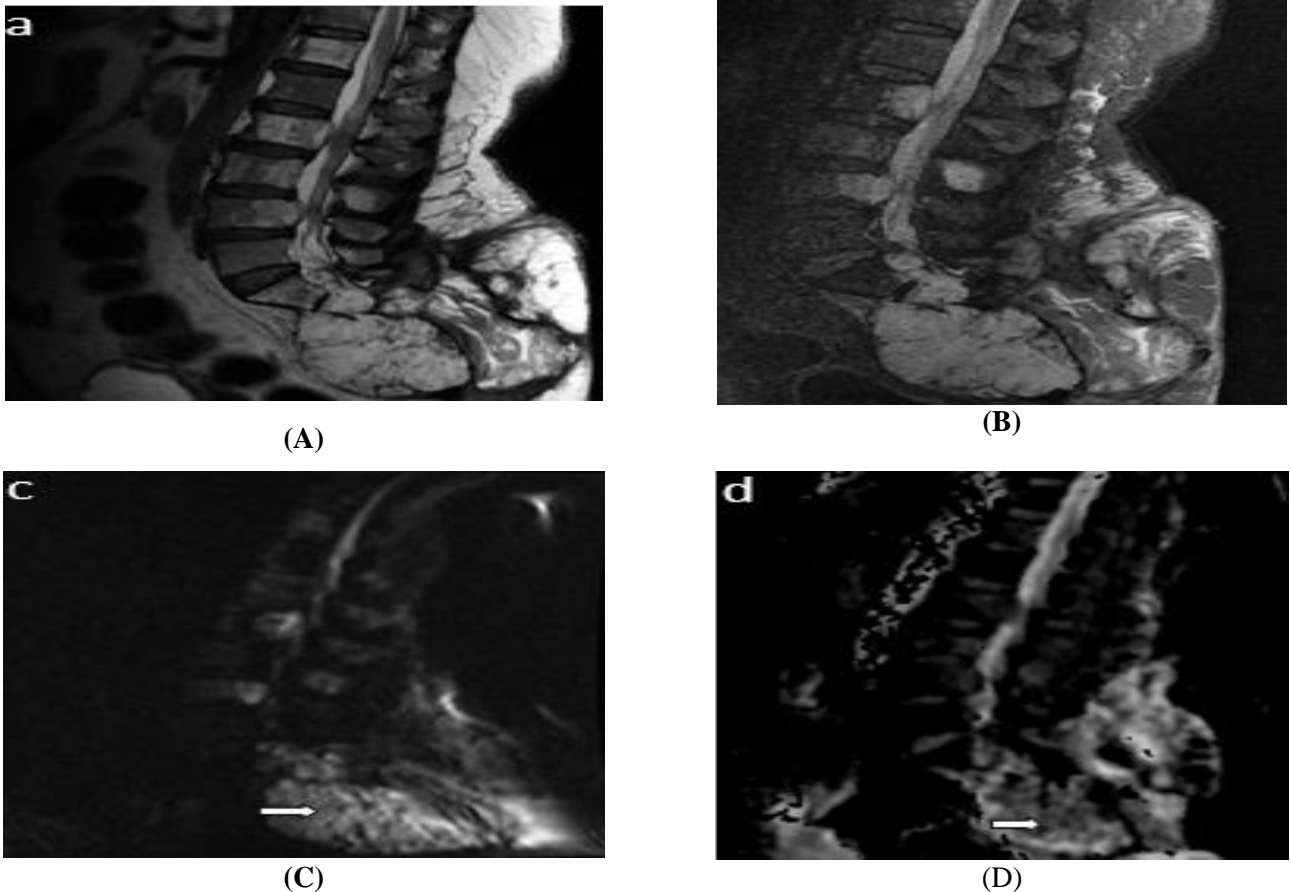


Figure (2): (A) Sagittal T2WI showed bony lesion with soft tissue component at sacrococcygeal region showed high T2 signal along with metastatic lesions at posterior part of vertebral bodies of L2 and L4 with high T2, (B) Sagittal short-time inversion recovery (STIR) showed bony lesion with soft tissue component at sacrococcygeal region that showed high signal along with metastatic lesions at posterior part of vertebral bodies of L2 and L4 with high signal, (C) Sagittal diffusion weighted imaging (DWI) showed heterogeneous high signal and (D) Apparent diffusion coefficient (ADC) map showed diffuse low signal with areas of high signal within the sacrococcygeal mass lesion with ADC value $1.22 \times 10^{-3} \text{ mm}^2/\text{s}$.

CASE 2

Female patient aged 60 years old suffering from back pain, bilateral lower limb weakness and numbness. A case of spondylodiscitis, potts disease (Figure 3).

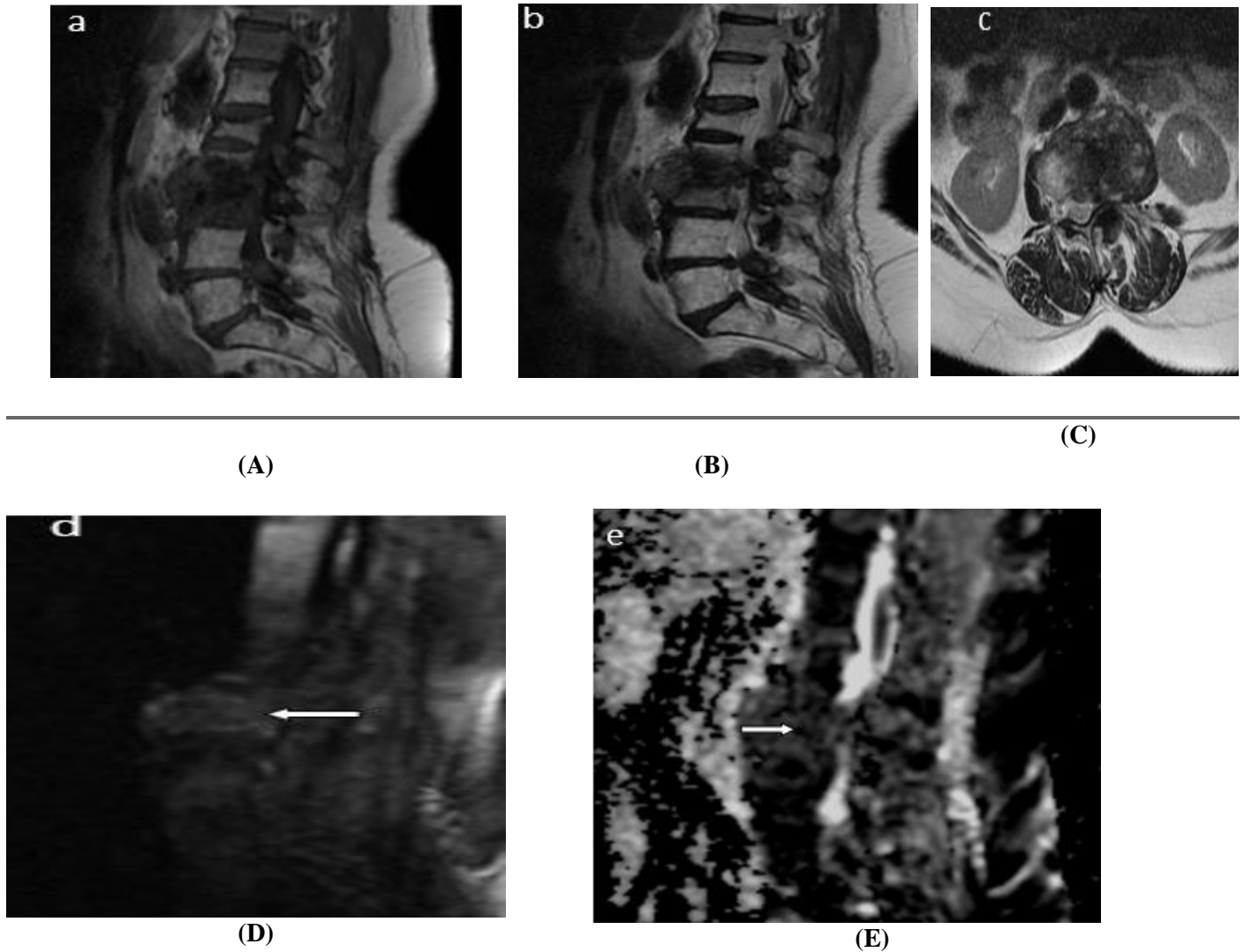


Figure (3): (A) Sagittal T1WI showed ill-defined lesion that was seen involving L2-3 opposing vertebral endplates as well as their intervertebral disc. It showed low T1 associated with prevertebral and left paravertebral component, (B) Sagittal T2WI showed mixed low and high T2, (C) Axial T2WI showed mixed low and high T2, (D) Sagittal diffusion weighted imaging (DWI) showed iso intense signal with areas of high signal in the affected vertebrae with high signal within the epidural collection and (E) Sagittal apparent diffusion coefficient (ADC) showed low signal within the epidural collection with ADC value of $1.27\text{mm}^2/\text{s}$.

CASE 3

Male patients aged 55 years old suffering from back pain (Figure 4).

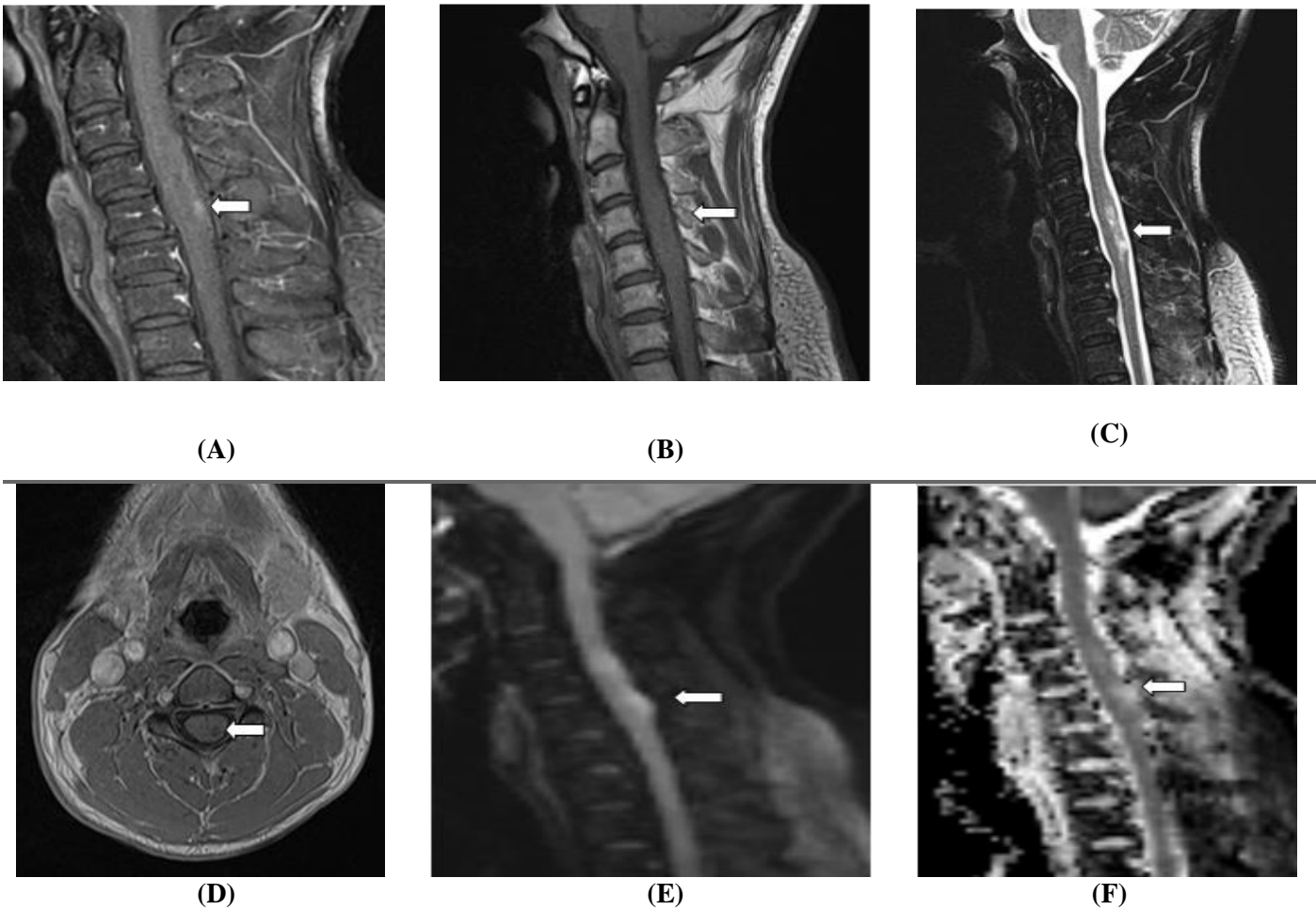


Figure (4): Sagittal T1WI showed expanding cervical cord at the level of C4 and C5 (B) Sagittal T2WI showed an intramedullary multifocal lesion that was seen along the posterior aspect of the cervical cord opposite C4 and C5 measured $2.8 \times 0.6 \text{ cm}$ and having hyperintense signal at T2 (white arrow), (C) and (D) Sagittal and axial post-contrast T1 fat sat showed nodular post-contrast enhancement of the lesion, (E) Sagittal DWI showed hyperintense signal of the lesion (restricted diffusion) and (f) Sagittal ADC map showed relative persistence of the high signal with ADC value of the lesion measured $1.12 \times 10^{-3} \text{ mm}^2/\text{s}$.

DISCUSSION

Lesions within the spinal canal can be categorized into neoplastic and non-neoplastic types. The non-neoplastic lesions included various conditions such as vascular, inflammatory, developmental, demyelinating, degenerative, metabolic, and toxic disorders [1]. Neoplastic lesions are further classified according to their anatomical location relative to the spinal cord, distinguishing between extradural, intradural extramedullary, and intramedullary intradural types [2].

Among the several diagnostic procedures for spinal illnesses, the MRI scan is considered the most suitable tool for physicians in their everyday practice. This technique has a superior level of detail and effectively displays both the skeletal and soft tissue components of

the spinal canal. As a result, it allows for accurate assessment of the disease's severity [13].

In this study, the lesions were found located lumbar (36.7%), cervical (33.3%), dorsal (20%), lumbosacral (6.7%), and sacrococcygeal (3.3%). Similar predominance of lumbar and cervical lesions was reported in the study of Allam *et al.* [11]. The higher prevalence of lesions in the lumbar region could be because the lumbar spine supports a substantial amount of the body's weight and is involved in a wide range of movements.

Concerning the final pathological diagnosis, the final pathological diagnosis of the studied patients, twenty-two patients had benign lesions (73.3%), while 8 patients had malignant lesions (26.7%). Concerning

tissue types, the most prevalent benign lesion was hemangioma (13.3%), and the most prevalent malignant lesion was metastasis (23.3%). The primary sites for metastasis were HCC (6.7%), breast cancer (3.3%), bronchogenic carcinoma (3.3%), cancer colon (3.3%), sinus melanoma (3.3%), and thyroid carcinoma (3.3%). In line with our study, **Ciftdemir et al.** [14] determined that the prevalence of hemangiomas and enostoses, that are considered the most frequent primary tumors of the spine, ranges from 11% to 14%. As for the malignant lesions and the predominance of metastatic lesions, consistent data was reported by **Fridley et al.** [15] highlighted that metastatic spine disease is quite common.

According to the results of this study, routine MRI sequences were non-specific in lesion characterization, with no substantial variation found among the patients with benign and malignant lesions in the lesion appearance and signal intensity. This agrees with other studies of **Soto-Subiabre et al.** [16], and **Mohamed et al.** [17] who confirmed the non-specificity of routine sequences.

DWI is a widely used MRI method that measures the movement of water molecules in biological tissues. By analyzing the MR signal intensity, DWI may provide details about the microscopic structure and organization of tissues, allowing for the detection of different pathological alterations in organs or tissues [18]. Lesion visual evaluation in this study was mainly on the high b-value (800 mm²/s) images, as it was considered that qualitative evaluation of DWI and ADC images on low b-value will allow the overestimation of the diffusion effect due to the contribution of perfusion to the signal attenuation [19].

In this study, malignant lesion had statistically significant higher diffusion restriction as appeared from the DWI, and from the ADC (10-3 mm²/s) values (0.99 ± 0.14 compared to 1.62 ± 0.35 in benign lesions). This comes in agreement with other studies that reported that significant higher rates of diffusion restriction were associated with malignancy [16, 17, 20].

Using ROC analysis, we identified the validity of ADC to discriminate malignant masses. ADC (10-3 mm²/s) values showed significant predictive value of the malignant lesions. An ADC cutoff value of ≤ 1.25 could predict malignant lesions with a sensitivity of 88.5% and specificity of 92.4%. The cutoff value obtained from the current work is in the range reported by other studies. In the study of **Allam et al.** [11], ADC demonstrated substantial predictive capability in identifying malignant lesions when the cutoff value was set at ≤ 0.9 × 10⁻³. The sensitivity and specificity of this cutoff were 85.7% and 91.3%, respectively. According to **Taskin et al.** [21], the optimal cutoff value of 1.32 × 10⁻³ mm²/s could distinguish benign and malignant spinal lesions. The sensitivity and specificity were determined to be 96.5% and 95.2%, respectively, while the positive and negative predictive values were

also found to be 96.5% and 95.2% respectively. **Abo Dewan et al.** [22] achieved a sensitivity of 95.12% and specificity of 92.73% in distinguishing between malignant and benign lesions with a positive predictive value of 90.70% and a negative predictive value of 96.23% for differentiating benign and malignant spinal lesions using an optimal cutoff value of 1.21 × 10⁻³ mm²/s. In accordance with **Taskin et al.** [23], the best cutoff value of 1.32 × 10⁻³ mm²/s was obtained for differentiating between benign and malignant spinal lesions. The sensitivity was found to be 96.5%, specificity was 95.2%, positive predictive value was 96.5%, and negative predictive value was 95.2%. **Kaur et al.** [24] successfully differentiated between benign and malignant diseases utilizing quantitative DW-ADC maps. They achieved high levels of sensitivity, specificity, positive predictive value, and negative predictive value by using a threshold value of 1.21 × 10⁻³ mm²/s.

The variability observed in the reported cutoff values for ADC across different studies can be attributed to a combination of factors inherent to the study design and the underlying characteristics of the patient populations. These variations underscore the complexity and nuances of interpreting diagnostic test results within the context of different clinical scenarios. The disease spectrum under investigation also plays a pivotal role. The imaging techniques employed in different studies can introduce technical variability in ADC measurements. Variations in imaging protocols, such as MRI machine type, field strength, and specific imaging sequences, can influence ADC values.

The limitations of our study were that the sample size was relatively small and that the study was done in a single center.

CONCLUSION

Spinal canal lesions encompass a wide range of neoplastic and non-neoplastic conditions, posing diagnostic challenges due to their often-similar appearance on routine MRI sequences. This finding is consistent with previous research and underscores the potential of DWI as an essential diagnostic tool in spinal canal lesion characterization.

Financial support and sponsorship: Nil.

Conflict of Interest: Nil.

REFERENCES

1. **Kettner M, Udelhoven A (2021)** :Nonneoplastic lesions of the spinal canal. *Radiol.*, 61:283-290.
2. **Walha S, Fairbanks S (2021)**: Spinal cord tumor surgery. *Anesthesiol Clin* .,39:139-149.
3. **Yáñez M, Miller J, Batchelor T(2017)**: Diagnosis and treatment of epidural metastases. *Cancer* ,123:1106-1114.
4. **Koeller K, Shih R (2019)**: Intradural Extramedullary Spinal Neoplasms: Radiologic-Pathologic Correlation. *Radiographics* ,39:468-490.

5. Ulbrich E, Schraner C, Boesch C *et al.* (2014): Normative MR cervical spinal canal dimensions. *Radiol.*, 271:172-182.
6. Rutges J, Kwon B, Heran M, Ailon T, Street J, Dvorak M (2017): A prospective serial MRI study following acute traumatic cervical spinal cord injury. *Eur Spine J.*, 26:2324-2332.
7. Nguyen T, Thelen J, Bhatt A (2020): Bone up on spinal osseous lesions: a case review series. *Insights Imaging*, 11:80-96.
8. Filograna L, Magarelli N, Cellini F *et al.* (2018): Diffusion weighted imaging (DWI) and apparent diffusion coefficient (ADC) values for detection of malignant vertebral bone marrow lesions. *Eur Rev Med Pharmacol Sci.*, 22:590-597.
9. Baliyan V, Das C, Sharma R, Gupta A (2016): Diffusion weighted imaging: Technique and applications. *World J Radiol.*, 8:785-798.
10. Tanenbaum L (2013): Clinical applications of diffusion imaging in the spine. *Magn Reson Imaging Clin N Am.*, 21:299-320.
11. Allam K, Abd Elkhalek Y, Hassan H, Emara M (2022): Diffusion-weighted magnetic resonance imaging in differentiation between different vertebral lesions using ADC mapping as a quantitative assessment tool. *Egypt J Radiol Nucl .*,53:155-260.
12. Mahmood F, Hansen R (2017): Diffusion Weighted Magnetic Resonance Imaging for Detection of Tissue Electroporation In Vivo. In: Miklavčič D, editor. *Handbook of Electroporation*. 44. 2nd ed. Cham: Springer International Publishing; 2017:723-743.
13. Tadros M, Louka A (2016): Discrimination between benign and malignant in vertebral marrow lesions with diffusion weighted MRI and chemical shift. *Egypt J Radiol Nucl.*, 47:557-569.
14. Ciftdemir M, Kaya M, Selcuk E, Yalniz E (2016): Tumors of the spine. *World J Orthop.*, 7:109-116.
15. Fridley J, Syed S, Niu T, Leary O, Gokaslan Z (2020): Presentation of spinal cord and column tumors. *Neuro-Oncology Practice*, 7:18-24.
16. Soto-Subiabre M, Mayoral V, Fiter J, Valencia L, Subirana I, Gómez-Vaquero C (2020): Vertebral fracture: clinical presentation and severity are linked to fracture risk factors. *Osteoporos Int.*, 31:1759-1768.
17. Mohamed A, Nardine N, Mohamed T, Amr Y (2018): Role of Diffusion Weighted Magnetic Resonance Imaging in Differentiation between Benign and Malignant Vertebral Body Collapse. *The Medical Journal of Cairo University*, 86:867-873.
18. Baliyan V, Das C, Sharma R, Gupta A (2016): Diffusion weighted imaging: technique and applications. *World journal of radiology*, 8:785.
19. Yeung D, Wong S, Griffith J, Lau E (2004): Bone marrow diffusion in osteoporosis: evaluation with quantitative MR diffusion imaging. *J Magn Reson Imaging*, 19:222-228.
20. Karaarslan E, Arslan A (2008): Diffusion weighted MR imaging in non-infarct lesions of the brain. *Eur J Radiol.*, 65:402-416.
21. Taşkın G, İncesu L, Aslan K (2013): The value of apparent diffusion coefficient measurements in the differential diagnosis of vertebral bone marrow lesions. *Turk J Med Sci.*, 43:379-387.
22. Dewan K, Salama A, Khalil A (2015): Evaluation of benign and malignant vertebral lesions with diffusion weighted magnetic resonance imaging and apparent diffusion coefficient measurements. *The Egyptian Journal of Radiology and Nuclear Medicine*, 46:423-433.
23. Taşkın G, İncesu L, Aslan K (2013): The value of apparent diffusion coefficient measurements in the differential diagnosis of vertebral bone marrow lesions. *Turkish Journal of Medical Sciences*, 43:379-387.
24. Kaur A, Thukral C, Khanna G, Singh P (2020): Role of diffusion-weighted magnetic resonance imaging in the evaluation of vertebral bone marrow lesions. *Pol J Radiol.*, 85:215-223.